Image analysis characterization of the lymph/angiogenesis in experimental models and clinical studies

Cedric Balsat[1], *Silvia Blacher*[1], *Nicolas Singolle*[1], *Frédéric Kridelka*[2], *Agnes Noël*[1]
[1]*Laboratory of Tumor and Developmental Biology, University of Liège, Tour de Pathologie (B23), Sart-Tilman; B-4000 Liège*
[2]*Department of Obstetrics and Gynecology, CHU of Liège, B-4000 Liège*

Email: cedric.balsat@chu.ulg.ac.be

Keywords
Lymph/angiogenesis, detailed characterization, improvement

Introduction

Lymph/angiogenesis, i.e. the formation of new lymphatic/blood vessels from pre-existing ones, strongly focus the interest of researchers and clinicians since they have been associated with cancer progression and metastasis [1, 2]. Several assays are widely used by biologists to study the evolution of these mechanisms as well as the efficiency of anti-lymph/angiogenesis compound. In most studies, qualitative and/or semi-quantitative measurements are based on visual descriptions, manual vessel/cell counting or global densities. In this work, image analysis methods are applied to quantify the structure of experimental models and clinical samples. It is shown that it provides an accurate quantitative description of both morphological and spatial modifications of the lymphatic/blood vessels architecture in function of their microenvironment.

Materials and Methods

We have developed **original possessing** software allowing an automatic segmentation of lymphatic/blood vessels/cells as well as generated **new quantification methods** to perform a detailed analysis of morphological modifications and spatial vessel distribution. These systems have been developed to be applied in virtual images acquired by a scanner coupled with a high resolution camera and/or optical microscopes (i.e. fluorescent and visible) in ***in vivo*** (Figure 1) and ***in vitro*** (Figure 2) models as well as on **clinical samples** (Figure 3) indiscrimina

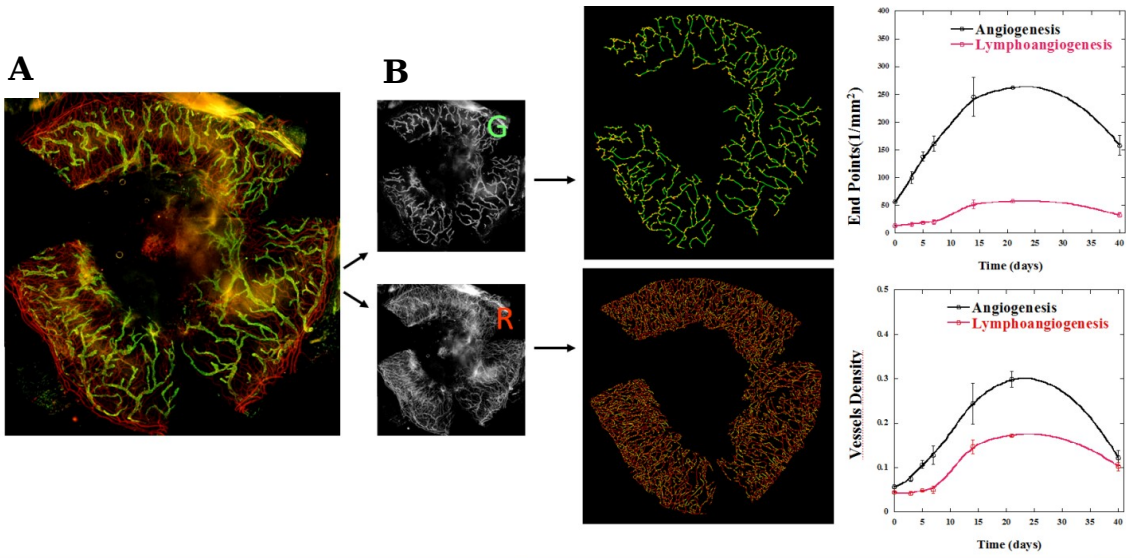

Eric Pirard

Figure 1: Image processing and measurements developed to study the corneal lymph/angiogenesis development after thermal cauterization. (A) Corneal vascular network 14 days after thermal cauterization. Blood (red) and lymphatic (green) vessels are evidenced by whole-mount immunostaining directed against CD31 and LYVE-1 respectively. (B)Splitting RGB channels to dissociate blood (R) from lymphatic vessels (G). (C) Segmentation, skeletisation and detection of end points (sprout tips) and branchings for blood and lymphatic vessels. (D) Time evolution of the number of sprout tips (top graph) and total vessel (botton graph) densities of the blood (black curve) and lymphatic (red curve) neoformed vessels.

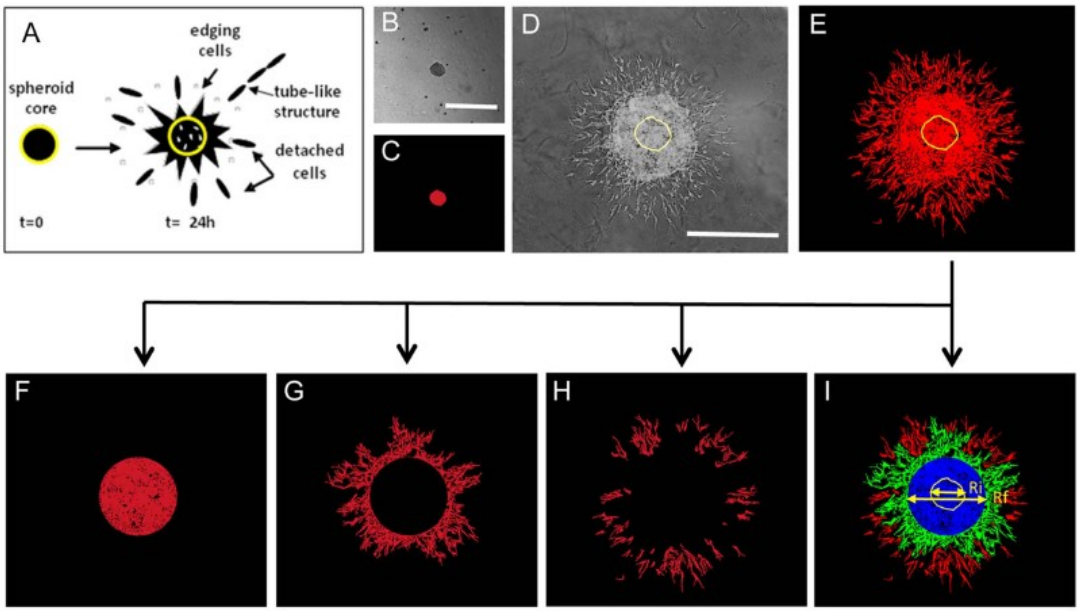

L

	Measurements	t=0	t=24
Global Measurements	Mean Envelope Area (mm^2)	0.02	0.61
	Mean Total Cell Area (mm^2)	0.02	0.24
	d_1 (mm)= R_i	R_i =0.08	0.44
	d_2 (mm)	-	0.23
	R_f (mm)	-	0.21
Local Measurements	Mean Core Cell Area (mm^2)	0.02	0.10
	Mean Edging Cell Area (mm^2)	-	0.09
	Mean Detached Cell Area (mm^2)	-	0.14

Figure 2: Image processing and quantification of *in vitro* lymphatic endothelial cell spheroids. (A) Schematic representation of spheroid evolution during cell culture: core spheroid (yellow circle, left panel) and the different modes of cell migration after 24 h of culture (right panel). Representative images of spheroids after embedding into the collagen matrix at (B) t = 0h and (D) after 24 h of culture. (C, E) Corresponding binarised images.(F–H) Decomposition of the binarised image into three components: spheroid core (F), edging cells (G) and detached cells (H). (I) Representation of the whole spheroid and its components: the initial spheroid delineated by a yellow circle, the expanded spheroid core (blue), edging cells (green) and detached cells (red). (J) Illustration of the parameters used for global measurements: convex envelope (green) and total distance of cell invasion starting from the spheroid centre (d1) or border (d2). (K) Grid used for local measurements: a circular grid is superimposed on the coloured spheroid representation. (l) Comparison of global and local measurements at t = 0 and t = 24 h. (M) Graph representing the cell density distribution measured from the image. The colours of the curves correspond to the different spheroid components described in the other panels (A, I and K). Bars = 500 mm.

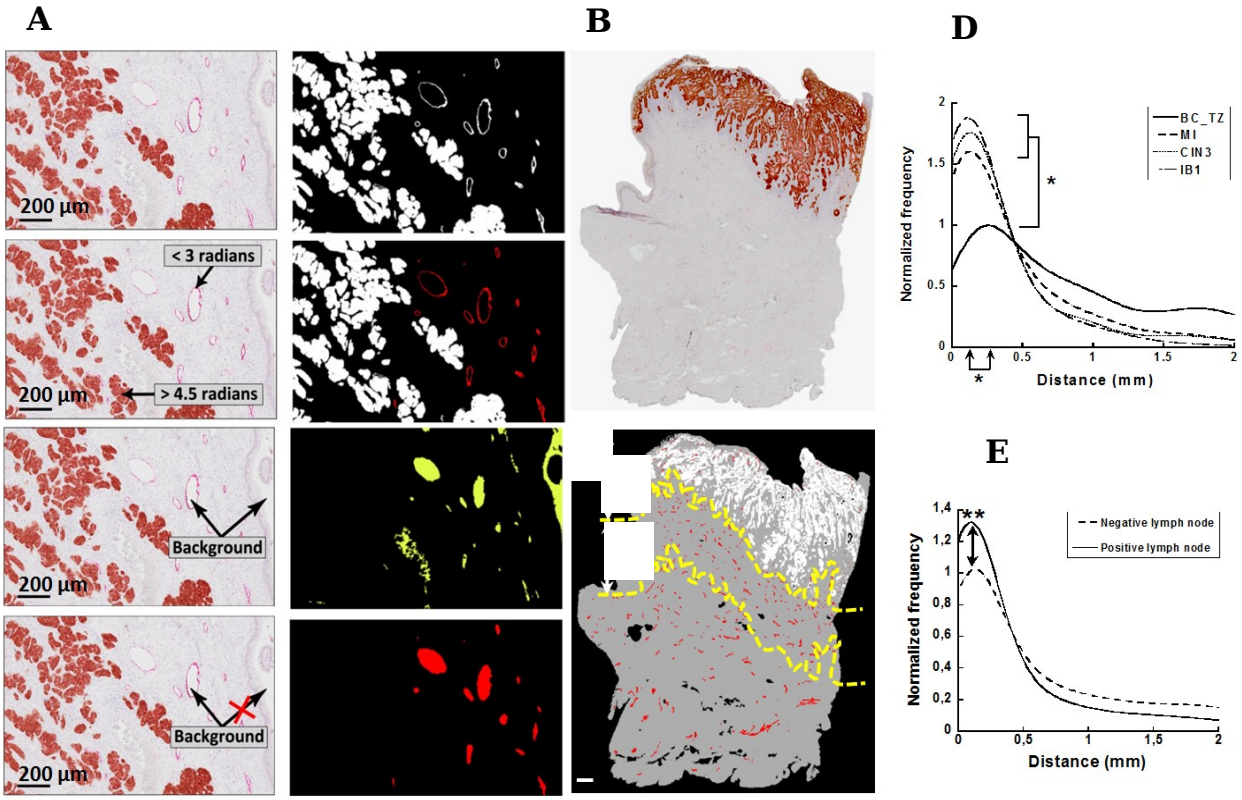

Figure 3: Image processing and quantification methodology developed to characterize the lymphatic vasculature on surgically collected human tissues. (A) Image processing illustration on digital images. Digital images of the immunostained tissue in which tumor cells (bruin) and lymphatic vessels endothelium (red) have been highlighted using antibodies directed against $P16^{ink4a}$ and podoblanin respectively (left column). Binary images of representing each steps of the segmentation procedure (right column). Segmentation was performed as follows (from the top downwards); (1) Lymphatic vessels and tumor cells were detected separately using appropriate thresholds. (2) Vessel lumens were segmented as the brightest values of the image (the threshold value depends on the average background value). To exclude blood vessel lumens or holes in the tissue, only lumens close to a red staining are kept. These two detections are gathered together. Finally a reconstruction by erosion is performed to remove small artifacts. (B) Virtual image acquisition of the whole tissue using with a full automated slide scanner (Olympus, dotslide). (C) Corresponding binary image obtained after the automated detection of tumor cells (white) lymphatic vessels (red) and the tissue (grey on whole slide. Intratumoral (i) and peritumoral regions (p) were manually discriminated (yellow dotted line). Graphs representing the quantification of the spatial lymphatic vessel distribution from the epithelial edges throughout cancer progression (top graph) and regarding the lymph node status (bottom graph). Spatial lymphatic vessel distribution analysis was performed by measuring the Euclidean distance between the center of mass of each vessel section and the epithelial edges.

Results and Discussion

In addition to classical quantifications of densities, new methodologies developed by our group allow us to perform a detail analysis of morphological and spatial evolution of lymphatic/blood vessels and cells. Another advantage of such methods rest with their capacity to perform, not only the investigation of a part of the *in vivo, in vitro* or clinical

systems studied, but also a characterization of biological processes in their entirety. Notably, in the corneal model, it is possibly to analyse simultaneously the structure and evolution of blood and lymphatic vessels. In the spheroid model, modifications of the spheroid core as well as the different kind of cell migration can be analysed. Finally, in the clinical study of the lymphatic vasculature, their spatial distribution around the tumor allowed to study their possible association with metastasis. Such analysis highlighted modifications that might be overlooked with classical methodologies

Conclusion

Development of new methodologies for the segmentation of vessels/cells and the quantification of morphological and spatial distribution parameters in *in vivo*, *in vitro* and clinical models has lead to a better characterization of how lymph/angiogenesis evolve. This represents a significant step toward a better understanding of the link existing between lymph/blood vessels and their microenvironment or tumor cells.

References

1. Quail, D.F. and J.A. Joyce, *Microenvironmental regulation of tumor progression and metastasis.* Nat Med, 2013. **19**(11): p. 1423-37.
2. Stacker, S.A., S.P. Williams, T. Karnezis, R. Shayan, S.B. Fox, and M.G. Achen, *Lymphangiogenesis and lymphatic vessel remodelling in cancer.* Nat Rev Cancer, 2014. **14**(3): p. 159-72.